Electromagnetic Analysis of a Novel Cylindrical Transverse-Flux Permanent-Magnet Linear Machine

Ping Zheng [1], Bin Yu [1], Haiyuan Yan [2], Yi Sui [1], Jingang Bai [1], and Pengfei Wang [1]

[1] School of Electrical Engineering and Automation
Harbin Institute of Technology, Harbin, 150080, China
zhengping@hit.edu.cn, yubin1983@163.com, suiyi_hitee2005@163.com, baijingangdiyi@163.com, and wpf6032@163.com

[2] China Academy of Launch Vehicle Technology, Beijing, 100076, China
yhylzx2005@sina.com

Abstract ─ Cylindrical transverse-flux permanent-magnet linear machine (TFPMLM) is a novel electric machine used for free piston energy converters. As the disadvantages of low power factor and complex manufacture exist in the conventional TFPMLM, this paper employs the staggered (not overlapped) stator teeth to reduce the flux leakage, and further increase the power factor and force density. In this paper the flux leakage and performances of two topologies are researched and compared. Then thorough analysis is made on axial 3-phase TFPMLM, which has great potential in force density and power factor. Thrust fluctuation, force density and power factor of the axial TFPMLM are analyzed. Moreover, the methods to improve force density and power factor are researched. Finally, a scheme with power factor up to 0.52, force density up to $2.17 \times 10^5 \text{N/m}^3$ is developed.

Index Terms ─ Flux leakage, force density, linear machine, power factor, and transverse flux.

I. INTRODUCTION

Transverse flux permanent-magnet machine (TFPMM) is a special structure PM machine. Unlike traditional machines, the electric load and magnetic load of TFPMM are decoupled from each other. High torque/force density can be obtained by improving the electric and/or magnetic load. So scholars make further research on the theory and technology of TFPMM, and great achievements have been made. TFPMM has broad prospect of application in wind power generation, marine propeller, linear drive, magnetic levitation, etc [1].

Since Professor H. Weh designed the first prototype of transverse flux machine (TFM), the later scholars have proposed a variety of different structures of transverse flux machines to improve the performance and the processing technology [2]. A TFM with C-shaped stator core was proposed by Rolls-Royce in Britain; the stator is made of soft magnetic composite (SMC), which has poor magnetic properties and high cost [3]. A C-core TFM was proposed by Royal Institute of Technology in Sweden, which has high power factor but low torque density [4]. An E-core TFM was proposed by Aalborg University in Denmark, which is suitable for high speed application because of the less pole number [5]. A TFM with claw-pole stator and outer rotor was proposed by Aachen Institute of Technology in Germany, which has small outer diameter, with liquid cooling used for heat dissipation [6]. Similar topology was investigated by the University of Southampton in UK [7]. A reluctance type TFM was proposed by the University of Calgary in Canada, which has simple manufacturing process, but increases the amount of permanent magnets [8]. A TFM with permanent-magnet screen technology was proposed by the Electrotechnology Research Institute in Korea, which uses the permanent-magnet flux to weaken the leakage flux, and the machine performance is improved [9]. For TFMs, the problems of complicated structure, difficult manufacturability, and low power factor normally

exist. So a large number of researches have been developed on how to improve the power factor, simplify the structure, and optimize the parameters. The research work mainly focus on the application of new materials (SMC), optimal design methods (particle swarm design, magnetic field screen, and genetic algorithm), parameter optimizations (3-D finite element method, equivalent magnetic circuit method), control optimizations (harmonics current injection, symmetric current control), etc[10-15].

In this paper, a novel cylindrical transverse-flux permanent-magnet linear machine (TFPMLM) is proposed based on the previous research work on rectangular topology [16], which is used for a free-piston generator system. Cylindrical structure is more convenient to manufacture, and more suitable for assembling with the free-piston power generation system. Moreover, the novel cylindrical topology can solve the problems of high flux leakage and low power factor existing in the former rectangular one. Two different topologies are proposed and compared. The 3-D finite element method (FEM) (Maxwell 14.0) is used to simulate the flux distribution in different parts of the machine. With Armature and PM flux leakage considered, local optimization is used to find the best axial thickness of the stacked long stator core and pole arc coefficient. With power factor and force density considered together, parametric match optimization is used, with the combination of winding turns and pole number, the combination of air-gap length and axial length, and the overlapping cross-sectional angle of adjacent stator cores are investigated.

II. STRUCTURE AND LEAKAGE FACTOR OF THE NOVEL STAGGERED-TEETH CYLINDRICAL TFPMLM

A. Structure

Compared with traditional TFPMLM, the novel staggered-teeth cylindrical TFPMLM has a quite different stator structure. There are two kinds of arrangements of the machine structure, called axial 3-phase structure and circumferential 3-phase structure, respectively. For every pole pair, stator teeth are composed of three types of laminations arranged in the form of I, III, II, and III, successively, as shown in Figs. 1 (a) and 2 (a). I and II are defined as the stacked long stator core. Windings of each phase are wounded around the

roots of the teeth. Stator structure and mover structure are shown in Figs. 1 (b) and (c) and Figs. 2 (b) and (c), respectively. For 3-phase machine, the phase windings have two ways of arrangement, namely axial and circumferential 3-phase windings. For axial 3-phase structure, the adjacent phases are arranged by 2/3 pole pitch displacement in axial direction, as shown in Fig. 1 (d). For circumferential 3-phase structure, coils around two adjacent teeth forms a phase winding, and 3-phase windings are evenly distributed circumferentially, the PMs of the adjacent phases are arranged by 2/3 pole pitch displacement in the axial direction, as seen in Fig. 2 (d).
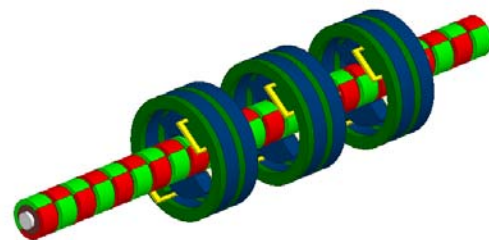

(a) Stator laminations.

(b) Stator structure.

(c) Mover structure.

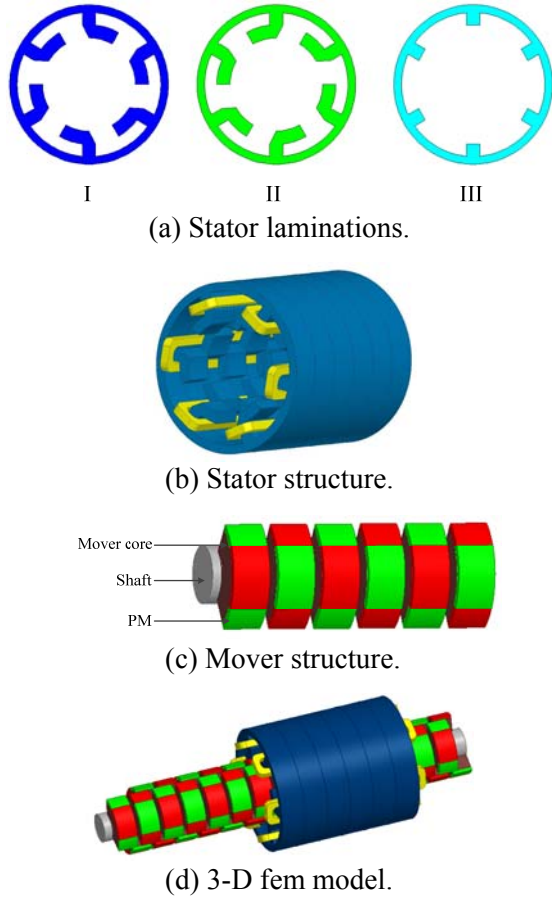(d) 3-D FEM model.

Fig. 1. Axial 3-phase structure.

(a) Stator laminations.

(b) Stator structure.

(c) Mover structure.

(d) 3-D fem model.

Fig. 2. Circumferential 3-phase structure.

B. General forms of flux leakage

There are PM flux leakage and armature flux leakage in TFPMLM. Leakage factor is defined as the ratio of the total flux and the main flux. Taking circumferential structure as an example, PM flux leakage includes flux leakage between transverse adjacent PMs, diagonal PM flux leakage between poles and flux leakage between longitudinal adjacent PMs, as in Fig. 3. Flux leakage between transverse adjacent PMs is defined as PM transverse leakage $\Phi_{\sigma pmt}$; the diagonal PM flux leakage between poles and the flux leakage between longitudinal adjacent PMs are defined as PM longitudinal leakage $\Phi_{\sigma pml}$. To calculate the leakage factor, the total flux and each flux leakage are calculated by 3D FEM, respectively. The flux leakage paths are shown by the solid arrow lines in Figs. 3 and 4. For each flux leakage, a yellow calculated plane is set up in the path of the flux leakage, and the flux leakage can be calculated by integrating the flux density on the plane. Both axial

thickness of stacked long stator core and arc coefficient play a significant role in the PM flux.

(a) Flux leakage between transverse adjacent PMs.

(b) Diagonal PM flux leakage between Poles.
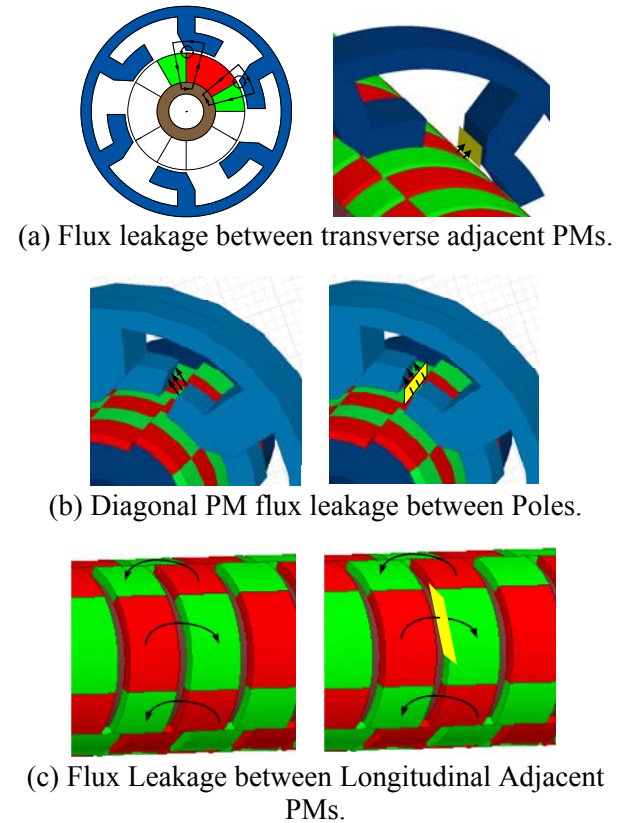

(c) Flux Leakage between Longitudinal Adjacent PMs.

Fig. 3. PM flux leakage paths and calculated planes.

Armature flux leakage includes slot flux leakage, flux leakage between teeth, and flux leakage between poles, as seen in Fig. 4. In addition, slot flux leakage and flux leakage between the teeth are defined as armature transverse leakage $\phi_{\sigma at}$; the flux leakage between poles is defined as armature longitudinal leakage $\phi_{\sigma al}$. Unlike PM flux leakage, armature flux leakage is mainly influenced by axial thickness of stacked long stator core.

(a) Slot flux leakage.

(b) Flux leakage between teeth.
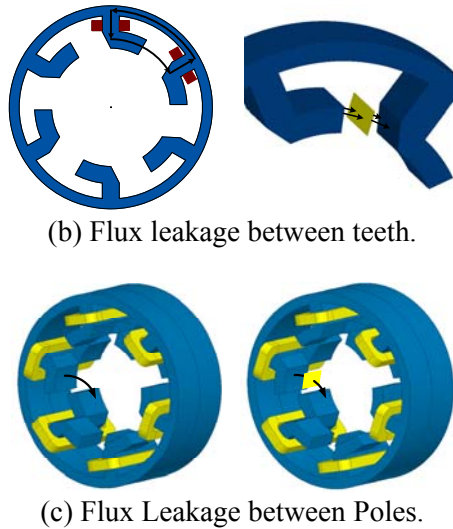

(c) Flux Leakage between Poles.
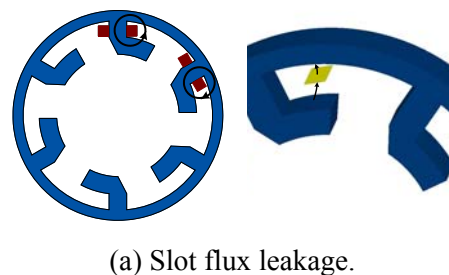
Fig. 4. Armature flux leakage paths and calculated planes.

C. Optimization of leakage factor

In this part, the topologies in Figs. 1 (d) and 2 (d) are optimized to reduce the flux leakage. Local optimization and FEM (provided by commercial software Maxwell 14.0) are used to find the best axial thickness of the stacked long stator core and pole arc coefficient.

1) *Optimization of the leakage factor of the axial three-phase type.*

The major parameters of the axial three-phase structure machine are shown in Table I.

Table I: Main parameters of axial three-phase type.

Parameters	Value	Parameters	Value
Rated power (kW)	1	Outer diameter of stator yoke	74mm
Rated velocity (m/s)	3	Inner diameter of stator yoke	60mm
Rated voltage(V)	44	Outer diameter of stator tooth	50mm
Material of the stator core	DW315-50	Inner diameter of stator tooth	26mm
Material of the mover core	DW315-50	Thickness of tooth	12mm
Permanent Magnet	N35SH	Length of air-gap	1mm
Winding	Single parallel-	Thickness of PM	3mm

	wounded concentrated winding		
Turns per phase	52	Outer diameter of mover	18mm
Slot fill factor	70%	Outer diameter of shaft	10mm
Number of poles per phase	16	Pole pitch	15mm

The following analysis is based on the condition that the pole pitch stays unchanged. The effect of thickness of the stacked long stator core on the armature flux leakage factor is analyzed when PMs are excluded, as shown in Fig. 5. While Fig. 6 shows the effect of thickness of the stacked long stator core on the PM flux leakage factor in the case that PM singularly produces flux.
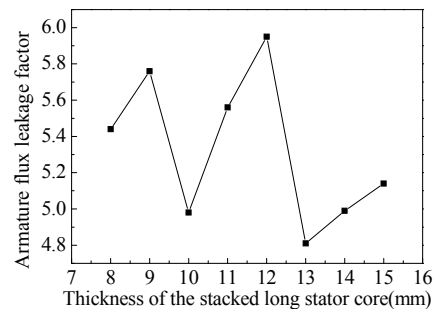

Fig. 5. Armature flux leakage factor versus axial thickness of the stacked long stator core.
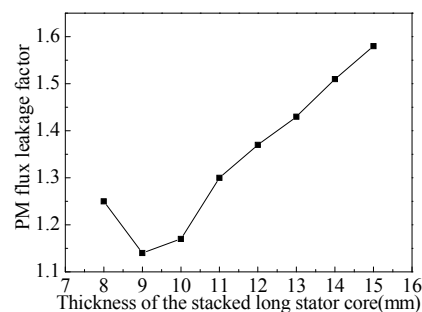

Fig. 6. PM flux leakage factor versus axial thickness of the stacked long stator core.

Considering the leakage factor of the armature and PM simultaneously, the axial thickness of the stacked long stator core is selected to be 10 mm.

The effect of arc coefficient on the PM flux leakage factor is shown in Fig. 7. It can be seen that with the increase of arc coefficient, PM longitudinal leakage increases, leading to an increase in the flux leakage factor. The PM flux leakage factor reaches a minimum of 1.17 when pole arc coefficient is 0.8, which is chosen to increase the PM utilization rate.
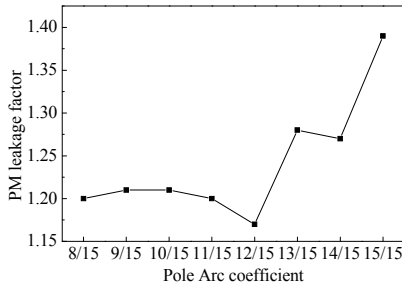

Fig. 7. PM flux leakage factor versus pole arc coefficient.

2) *Optimization of the leakage factor of circumferential three-phase type.*

The major parameters of the circumferential three-phase structure machine are shown in Table II.

Table II: Main parameters of the circumferential three-phase type.

Parameters	Value	Parameters	Value
Rated power (kW)	1	Outer diameter of stator yoke	78mm
Rated velocity (m/s)	3	Inner diameter of stator yoke	70mm
Rated Voltage(V)	44	Outer diameter of stator tooth	52mm
Material of the stator core	DW315-50	Inner diameter of stator tooth	42mm
Material of the mover core	DW315-50	Thickness of tooth	12mm
Permanent Magnet	N35SH	Length of air-gap	1mm
Winding	Single parallel-wounded concentrated winding	Thickness of PM	4mm
Turns per	35	Outer	36mm

phase		diameter of mover	
Slot fill factor	70%	Outer diameter of shaft	18mm
Number of poles per Phase	48	Pole pitch	15mm

Due to the same structure of the stator tooth per phase in the case of axial and circumferential structure, armature flux leakage of both is similar. While PM flux leakage factor of the two differs slightly because of the different PM arrangements. The effects of thickness of stacked long stator core on armature flux leakage factor and PM flux leakage factor are shown in Figs. 8 and 9, respectively. Considering the leakage factor of the armature and PM simultaneously, the axial thickness of the stacked long stator core is selected to be 12mm.
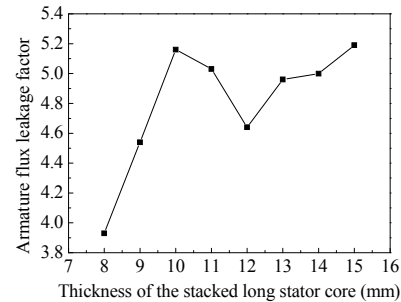

Fig. 8. Armature flux leakage factor versus axial thickness of the stacked long stator core.
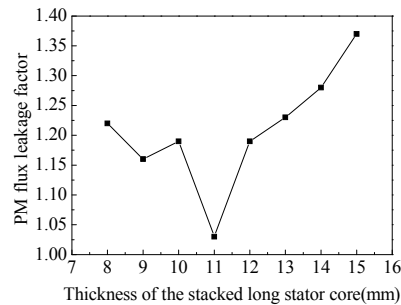

Fig. 9. PM flux leakage factor versus axial thickness of the stacked long stator core.

The trend of the PM leakage factor versus arc coefficient is shown in Fig. 10. Considering electromagnetic performances, pole arc coefficient is selected to be 12/15.
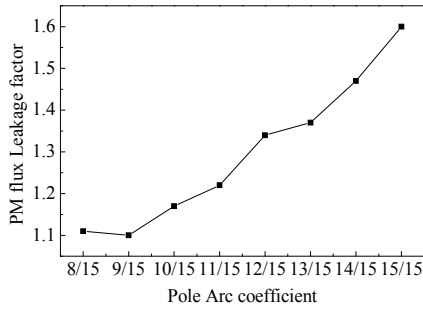
Fig. 10. The PM flux leakage factor versus the pole arc coefficient.

3) *Performance comparison between two structures.*

The key dimensions of the two types have been initially determined in the analysis above. In this part, simulation of no-load and load characteristics of the two types of machines is made by simplified 3-D FEM model, as realized in Figs. 1 (d) and 2 (d), and the results are shown as follows. The simplified model is based on equation (1),

$$E_{ph} = \sqrt{2}\pi f N p \Phi. \tag{1}$$

The thrust and back EMF of the simplified model and full model has the ratio of p_s/p, where p_s is the simplified pole pair number and p is the pole pair number in the full model. In this paper, p_s/p is 1/8. No-load characteristics of the two structures are shown in Figs. 11 and 12.

When the armature windings are fed with rated currents $I_N = I_q = 7.6$ A (d-axis current I_d is 0) and the mover moves at rated speed, load back EMF and thrust of the two structures are shown in Figs. 13 and 14. To make a clear comparison, some key performances are listed in Table III.
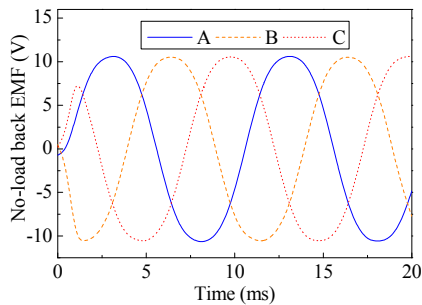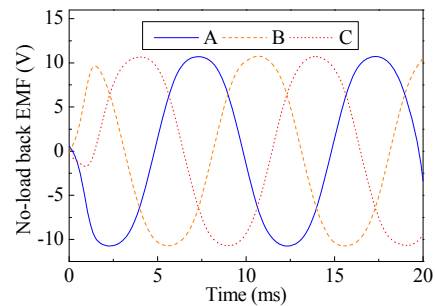
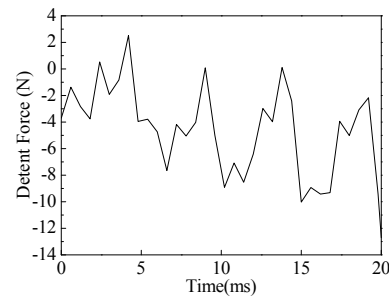

(a) No-load back EMF.
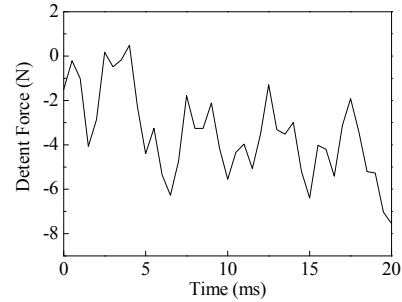
(b) Detent force.

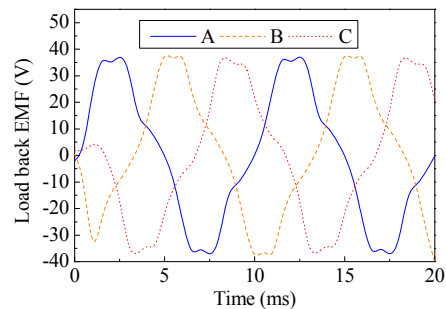Fig. 11. No-load performance of the axial 3-phase structure.

(a) No-load back EMF.

(b) Detent force.

Fig. 12. No-load performance of circumference 3-phase structure.
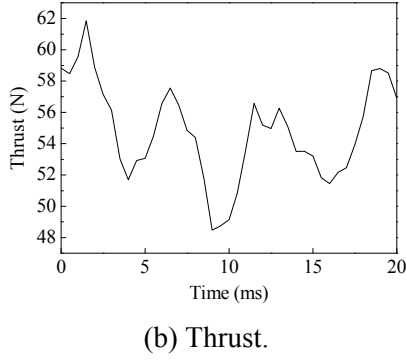

(a) Load back EMF.

(b) Thrust.

Fig. 13. Load performance of the axial 3-phase structure.
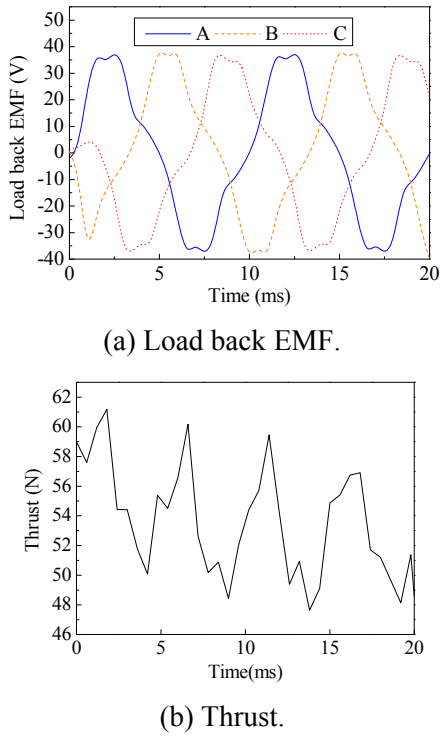
(a) Load back EMF.

(b) Thrust.

Fig. 14. Load performance of the circumference 3-phase structure.

Table III: Performance comparison of the two structures.

	Axial 3-phase type	Circumferential 3-phase type
the aberration rate of no-load EMF	0.0667	0.3137
Detent force	3.46	4.45
Thrust fluctuation	12.12%	12.44%
Force density(N/m^3)	1.40×10^5	4.17×10^4

Compared with the circumferential structure, the axial counterpart has a lower back EMF aberration rate and detent force, but has almost the same thrust fluctuation. The latter also has a higher force density. Therefore, axial 3-phase type is chosen for further study.

III. THRUST FLUCTUATION, FORCE DENSITY AND POWER FACTOR OF AXIAL TFPMLM

A. Theoretical analysis

From the previous analysis, thrust fluctuation is as high as 12.12 % for axial structure. Thrust fluctuation results in the vibration and noise of the machine, and especially in the case of low speed, resonance [17].

Detent force is the key indicator of thrust fluctuation. For normal linear machines, detent force can be decreased by modifying the pole pitches of stator and mover [18, 19]. While in the proposed machine, this method becomes useless because the pole pitch of the stator equals to that of the mover. The decrease of the detent force can be achieved by changing the arc coefficient, since the distribution of the harmonic magnetic field varies with arc coefficient significantly.

Being the primary concern of the novel cylindrical TFPMLM, force density and power factor are analyzed for axial structure by deducing the formulae of force density and power factor. Thrust is given by equation (2),

$$F = \frac{3\sqrt{2}\pi^2}{8} NpB_\delta J \frac{l_s}{\tau} D_{si} S_c \cos\varphi. \quad (2)$$

The symbol N is the turns-in-series per-phase, p is pole pair number, B_δ is air gap flux density, τ is the pole pitch, l_s is axial length of PM, D_{si} is the inner diameter of the stator, and S_c is the cross-sectional area of the conductor. The force density is given by equation (3),

$$F_\xi = \frac{F}{p\tau\pi(\frac{D_o^2}{4})} = \frac{3\sqrt{2}\pi}{2} NJB_\delta \frac{l_s}{\tau} \frac{D_{si} S_c \cos\varphi}{D_o^2 \tau}. \quad (3)$$

The symbol D_o refers to the outer diameter of the stator. The power factor is defined by equation (4),

$$\cos\varphi = \frac{E_{ph}}{\sqrt{E_{ph}^2 + (\omega L I_q)^2}}. \quad (4)$$

Where E_{ph} is the phase back EMF. The power factor can be further derived as shown in equation (5),

$$\cos\varphi = \frac{1}{\sqrt{1 + \dfrac{32(\omega L I_q)^2}{\pi^4 (NpB_\delta vD_{si} \dfrac{l_s}{\tau})^2}}}. \qquad (5)$$

From equations (3) and (5), it is obvious that the force density and the power factor depends on l_s/τ, i.e., the pole arc coefficient α. In condition that the pole arc coefficient remains constant, the axial thickness of the stacked long stator core affects the force density via utilization ratio of the PM and power factor via the armature flux leakage.

B. 3D-FEM simulation

When the axial thickness of the stacked long stator core stays 10 mm, no-load and load performances with different pole-arc coefficients are shown in Figs. 15, 16, and 17, respectively. The aberration rate of the no-load EMF and decent force decrease firstly, and then increase.
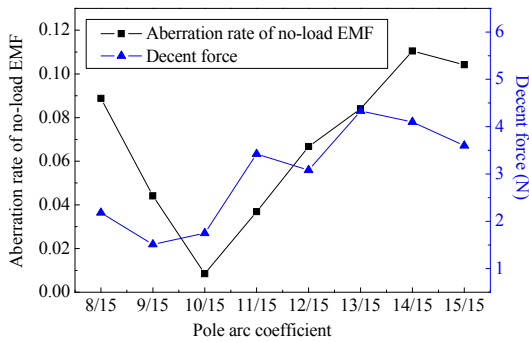

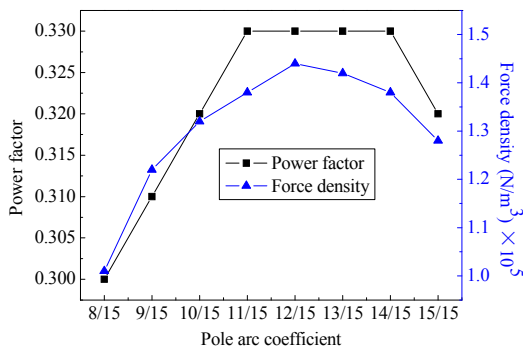Fig. 15. The decent force and aberration rate of no-load EMF versus pole arc coefficient.

Fig. 16. Power factor and force density versus pole-arc coefficient.

The force density and power factor increase firstly, and then decrease. It can be seen that favorable no-load and load performances are achieved when pole arc coefficient is 12/15.
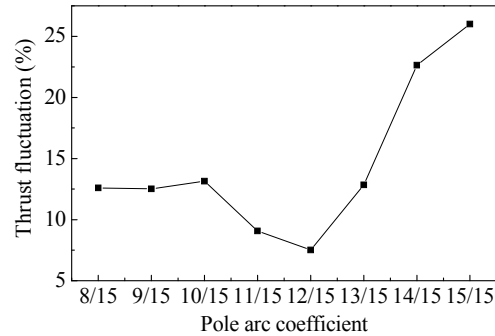

Fig. 17. Thrust fluctuation versus pole arc coefficient.

When the pole arc coefficient stays 12/15 and the axial thickness of the stacked long stator core ranges from 8 mm to 15 mm, the performances of no-load are shown in Fig. 18. The aberration rate of no-load EMF increases at first, and then decreases; the decent force has the opposite phenomena. When the axial thickness of the stacked long stator core ranges from 8 mm to 15 mm, the performances of the load are shown in Fig. 19. The force density firstly increases, and then decreases; the power factor has a descending trend. When the axial thickness of the stacked long stator core is 10 mm, the thrust fluctuation is the lowest, as shown in Fig. 20. With the performances of no-load and load taken into account, the axial thickness of the stacked long stator core is chosen to be 10 mm.
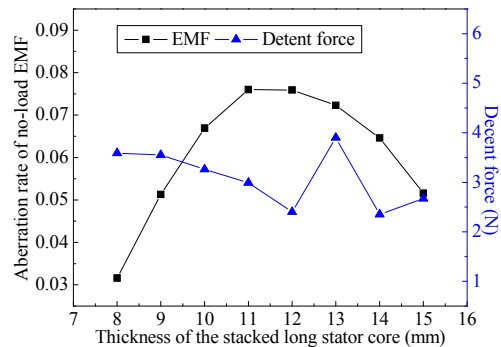

Fig. 18. The decent force and aberration rate of no-load EMF versus axial thickness of the stacked long stator core.
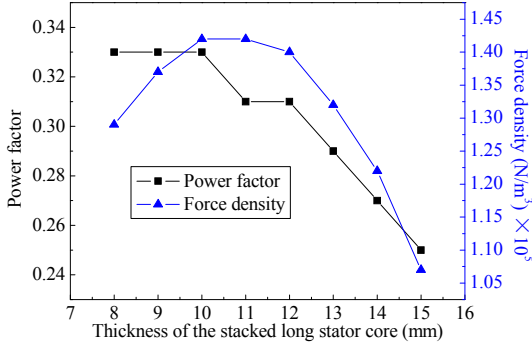
Fig. 19. Power factor and force density versus axial thickness of the stacked long stator core.
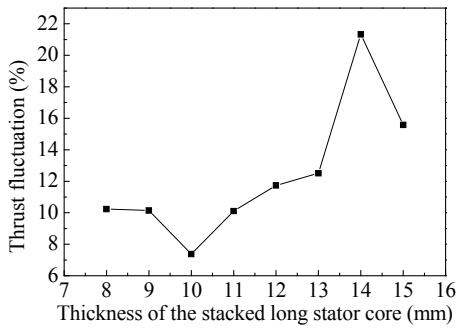

Fig. 20. Thrust fluctuation versus axial thickness of the stacked long stator core.

On the overall, when the pole-arc coefficient is 12/15 and axial thickness of the stacked long stator core is 10 mm, favorable no-load and load performances are achieved.

IV. THE METHODS TO IMPROVE FORCE DENSITY AND POWER FACTOR OF TFPMLM

Neglecting the saturation and armature reaction, thrust of the machine is given by equation (6),

$$F = m\frac{\sqrt{2}\pi p}{2\tau}\Phi_m N I_{ph}\cos\varphi. \qquad (6)$$

According to equation (6), there are three ways to improve the thrust of the preciously determined machine: increasing the air-gap flux Φ_m, increasing the armature current I_{ph}, and increasing the number of turns N. It is also necessary to take the effects on the power factor into account when implying the three methods. Power factor is determined by either equation (7) or (8) [20],

$$\cos\varphi = \cos[\tan^{-1}(\frac{\Phi_i}{\Phi_m})], \qquad (7)$$

$$\cos\varphi = \cos[\tan^{-1}(\frac{I_q X}{E_0})]. \qquad (8)$$

The symbol Φ_i is the flux that armature winding produces when armature current acts independently. The symbol Φ_m is the air-gap flux when permanent magnets act independently, X is the reactance, and E_o is the RMS value of no-load EMF. By increasing the air-gap flux Φ_m, the power factor and the force density can be increased at the same time. If the armature current I_{ph} is increased, the increased q-axis current I_q results in a lower power factor, though a higher force density can be achieved. Force density can be increased when the number of turns N is increased, but the power factor lowers dramatically as the reactance X is in proportion to the square of the number of turns N.

A. Combination of winding turns and pole number

According to the calculation results, the reactance X of the designed TFPMLM is 24.32 Ω, which is much larger than the reactance of the traditional radial-flux PM machine. Hence, a large reactance is another reason for the low power factor of TFPMLM. Besides, from equation (2) it is obvious that the number of pole pairs p needs to vary with the number of turns N in order to guarantee rated power output.

The 3D-FEM simulation results are shown in Fig. 21. It is easy to see that with the increase of the number of turns, the power factor decreases dramatically, while the force density has a very modest increase.
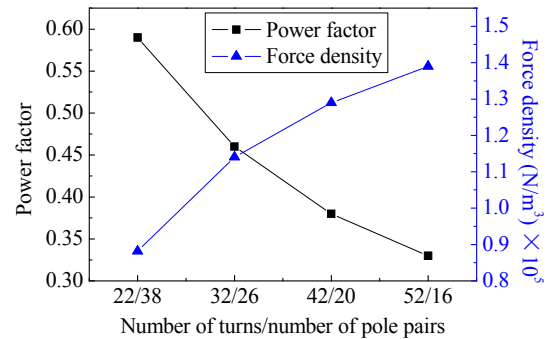

Fig. 21. Power factor and force density versus number of turns matching number of poles.

As a trade-off, the number of turns and pole pairs are chosen to be 32 and 26, respectively. And in this case, the power factor is 0.46 and the thrust density is $1.14 \times 10^5 \, \text{N/m}^3$.

B. Combination of air-gap length and axial length

As analyzed above, increasing Φ_m can increase the power factor and the force density simultaneously. The decrease of the air-gap length is the effective means of increasing Φ_m. A simplified FEM model for the pole-pair number being 2 and number of turns 32 is simulated. Similarly, the number of pole pairs varies with the change of air-gap length to guarantee rated power output. Figure 22 shows the trends of power factor and force density with regard to air-gap length.
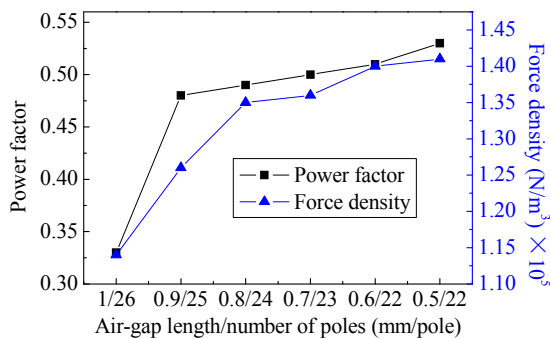

Fig. 22. Power factor and force density versus air-gap length matching number of poles.

It can be seen that the power factor and the force density both increase with the decrease of air-gap length. Thrust and thrust fluctuation are shown in Fig. 23. When the air-gap is 0.8 mm, thrust fluctuation is the lowest.
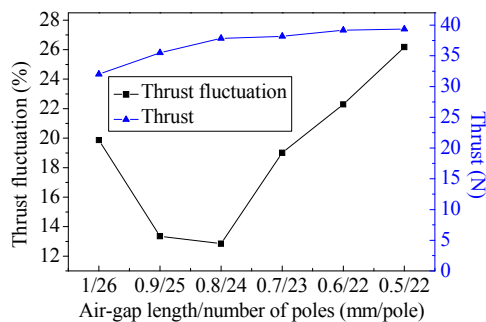

Fig. 23. Thrust fluctuation versus air-gap length / number of poles.

To ensure modest thrust fluctuation, the air-gap length is better to be 0.8 mm. The number of pole pairs is chosen to be 24. In this case, power factor is 0.49 and thrust density is $1.35 \times 10^5 \, \text{N/m}^3$.

C. Overlapping cross-sectional angle of adjacent stator cores

Overlapping cross-sectional angle of adjacent stator core is defined as θ as seen in Fig. 24, which can be optimized to get better power factor and force density. To reduce the axial armature-flux leakage, the adjacent stator teeth of the proposed machine are designed to be staggered. The accompanying problem is that the utilization ratio of PM is only 1/2. To compromise, overlapping cross-sectional angle of adjacent stator core can be optimized to get better power factor and force density, as is shown in Fig. 25.
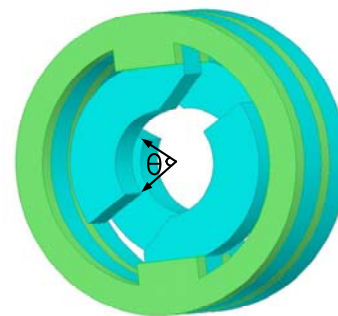

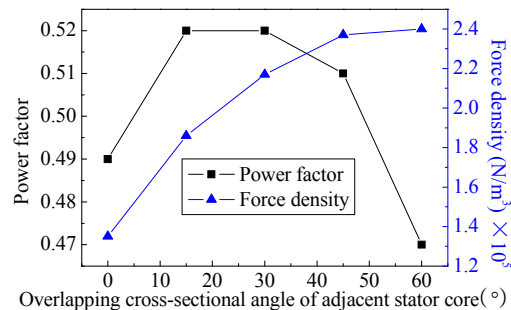Fig. 24. Overlapping cross-sectional angle of adjacent stator core.

Fig. 25. Power factor and force density versus overlapping cross-sectional angle of adjacent stator core.

It can be seen that the force density keeps increasing, while the power factor first increases to the largest value, and then decreases. That is because the axial armature-flux leakage increases dramatically when overlapping cross-sectional

angle of the adjacent stator core is too large. With the variation of the overlapping angle, thrust fluctuation is shown in Fig. 26. It is observed that the thrust fluctuation first decreases, and then increases. When overlapping cross-sectional angle of adjacent stator core is 15°, thrust fluctuation reaches a minimum value.

On the overall, in order to get high power factor and force density, θ is chosen to be 30°. The final model is simulated by 3-D FEM and the results are shown in Fig. 27. The final proposed TFPMLM has power factor of 0.52 and force density of 2.17×10^5 N/m^3. The efficiency of the designed TFPMLM is 88.3%. These performances are similar to most well-designed TFMs, but the machine structure in this paper is quite simple.
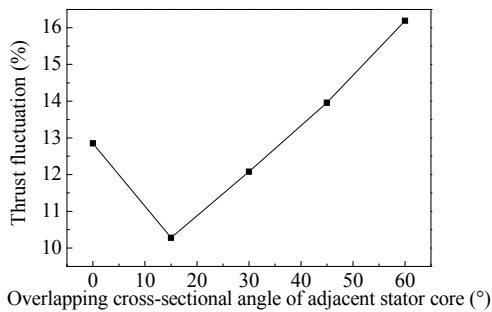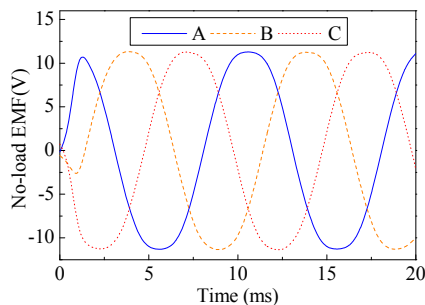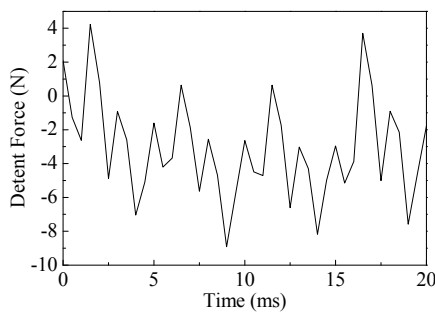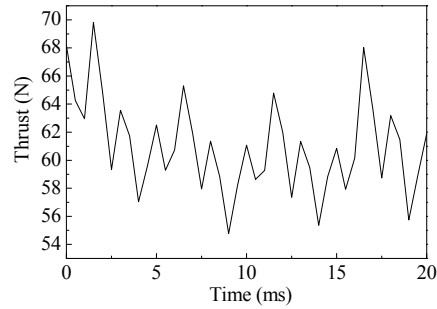

Fig. 26. Thrust fluctuation versus overlapping cross-sectional angle of adjacent stator core.

(a) No-load EMF.

(b) Detent force.

(c) Thrust.

Fig. 27. No-load and load performances of the final proposed TFPMLM.

V. CONCLUSION

A novel cylindrical transverse-flux permanent-magnet linear machine (TFPMLM) is proposed, which has axial 3-phase structure and circumferential 3-phase structure. The novel structure has the benefit of decreasing the flux leakage, which is the main factor that is affecting the performances of the TFPMLM. The axial 3-phase structure has better performances of back EMF and force density when compared to previous research. In the further study, a favorable scheme is achieved by optimizing the axial stacked stator core thickness and pole arc coefficient. In order to further improve the machine performance, the combination of number of turns and axial length, combination of air-gap length and axial length, and overlapping angle between adjacent stator teeth are reasonably matched. Finally, a scheme with power factor of 0.52, efficiency above 0.88 and force density up to 2.17×10^5 N/m^3 has been designed.

REFERENCES

[1] H. Polinder, B. Mecrow, A. Jack, P. Dickinson, and M. Mueller, "Conventional and TFPM linear generators for direct-drive wave energy conversion," *IEEE Trans. Energy Convers.*, vol. 20 , no. 2 , pp. 260-267, 2005.
[2] D. Kang and H. Weh, "Design of an integrated propulsion, guidance, and levitation system by magnetically excited transverse flux linear motor

(TFM-LM)," *IEEE Trans. Energy Convers.*, vol. 19, pp. 477-484, 2004.

[3] S. Husband and C. Hodge, "The Rolls-Royce transverse flux motor development," In *Proc. of IEEE International Electric Machines and Drives Conference (IEMDC2003)*, Madison, USA, pp. 1435-1441, June 2003.

[4] P. Anpalahan, J. Soulard, and H. P. Nee, "Design steps towards a high power factor transverse flux machine," In *Proc. of European Conference on Power Electronics and Applications*, Graz, Austria, pp. 1-6, August 2001.

[5] P. Rasmussen, G. Runolfsson, T. Thorsdottir, U. Jakobsen, and A. Pedersen, "E-core transverse flux machine with integrated fault detection system," *2011 International Conference on Electrical Machines and Systems (ICEMS2011)*, Beijing, China, pp. 1-6, August 2011.

[6] R. Blissenbach, I. Viorel, and G. Henneberger, "On the single-sided transverse flux machine design," *Electrical Machines and Power Systems*, vol. 31, no. 2, pp. 109-127, 2003.

[7] M. Harris and G. Pajooman, "Comparison of alternative topologies for VRPM (transverse-flux) electrical machines," *IEE Colloquium on New Topologies for Permanent Magnet Machines*, London, UK, pp. 2/1-2/7, June 1997.

[8] B. Hasubek and E. Nowicki, "Design limitations of reduced magnet material passive rotor transverse flux motors investigated using 3D finite element analysis," *2000 Canadian Conference on Electrical and Computer Engineering*, Halifax, NS, Canada, pp. 365-369, 2000.

[9] T. Hoang, D. Kang, and J. Lee, "Comparisons between various designs of transverse flux linear motor in terms of thrust force and normal force," *IEEE Trans. On Magn.*, vol. 46, no. 10, pp. 3795-3801, 2010.

[10] A. Shiri and A. Shoulaie, "Investigation of frequency effects on the performance of single-sided linear induction motor," *Applied Computational Electromagnetics Society (ACES) Journal*, vol. 27, no. 6, pp. 497-504, June 2012.

[11] H. Hasanien, "Particle swarm design optimization of transverse flux linear motor for weight reduction and improvement of thrust force," *IEEE Trans. Ind. Electron.*, vol. 58, pp. 4048-4056, 2011.

[12] Y. Nozaki, J. Baba, K. Shutoh, and E. Masada, "Improvement of transverse flux linear induction motors performances with third order harmonics current injection," *IEEE Trans. Appl. Supercon.*, vol. 14, pp. 1846-1849, 2004.

[13] D. Kang, "Increasing of thrust force in transverse flux machine by permanent-magnet screen," *IEEE Trans. On Magn.*, vol. 41, no. 5, pp.1952-1955, 2005.

[14] A. Argeseanu, E. Ritchie, and K. Leban, "Optimal design of the transverse flux machine using a fitted genetic algorithm with real parameters," *13th International Conference on Optimization of Electrical and Electronic Equipment*, Brasov, Romania, pp. 671-678, May 2012.

[15] J. Alwash and L. Qaseer, "Three-dimension finite element analysis of a helical motion induction motor," *Applied Computational Electromagnetics Society(ACES) Journal*, vol. 25, no. 8, pp. 703-712, August 2010.

[16] P. Zheng, C. Tong, G. Chen, R. Liu, Y. Sui, W. Shi, and S. Cheng, "Research on the magnetic characteristic of a novel transverse-flux PM linear machine used for free-piston energy converter," *IEEE Trans. On Magn.*, vol. 47, pp. 1082-1085, 2011.

[17] R. Nariman and S. Abbas, "Minimizing thrust fluctuation in linear permanent-magnet synchronous motor with Halbach array," In *Proceedings of Power Electronic & Drive Systems & Technologies Conference (1st PEDSTC)*, Tehran, Iran, pp. 302-306, Feb. 2010.

[18] A. Masnoudi and A. Elantably, "A simple assessment of the cogging torque in a transverse flux permanent magnet machine," In *Proceedings of IEEE International Electric Machines and Drives Conference (IEMDC2001)*, Cambridge, MA, USA, pp. 754-759, June 2001.

[19] A. Njeh, A. Masmoudi, and A. Elantably, "3D FEA based investigation of the cogging torque of a claw pole transverse flux permanent magnet machine," In *Proceedings of IEEE International Electric Machines and Drives Conference (IEMDC2003)*, Madison, USA, pp. 319-324, June 2003.

[20] M. Harris, G. Pajooman, and S. A. Sharkh, "The problem of power factor in VRPM (transverse-flux) machines," In *Proceedings of Eighth International Electric Machines and Drives Conference*, Cambridge, UK, pp. 386-390, Sep. 1997.

Ping Zheng (M'04–SM'05) received the B.Sc., M.Sc., and Ph.D. degrees from Harbin Institute of Technology, Harbin, China, in 1992, 1995, and 1999, respectively. Since 1995, she has been with Harbin Institute of Technology, where she has become a professor in 2005.

She is the member of IEEE IAS Electric Machines Committee, IEEE Industry Applications Society and International Compumag Society. Now she is an author or coauthor of more than 130 published refereed technical papers and four books. Her current research interests include electric machines and control, hybrid electric vehicles, and unconventional electromagnetic devices.

Bin Yu received the B.Sc. degree in Electrical Engineering from Tianjin University of Science and Technology in 2005, and M.Sc. degree from North China Electric Power University in 2010. He is currently working for his Ph.D. degree in Harbin Institute of Technology, China. His research interests include the design and control of new-structure permanent-magnet linear machines for free-piston stirling engines and series hybrid electric vehicles.
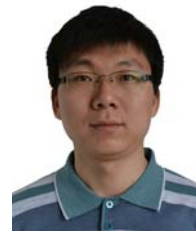
Haiyuan Yan received the B.Sc. degree and the M.Sc. degree in Electrical Engineering and Automation from Harbin Institute of Technology, Harbin, China, in 2009 and 2011. After her graduation, she worked in China Academy of Launch Vehicle Technology, dedicating to electromechanical servo technology research. Her research interests include transverse flux permanent magnet linear generator used in stirling system, permanent magnet synchronous servo motor used in electromechanical servo system of rockets and missiles, and the servo control technology of PMSM.

Yi Sui received the B.Sc. degree and M.Sc. degree in Electrical Engineering from Harbin Institute of Technology, Harbin, China, in 2009 and 2011, respectively. He is currently working toward the Ph.D. degree. His research interests include fault-tolerant permanent-magnet synchronous machine system used in pure electric vehicles, permanent-magnet linear machines, and high performance servo machine system used in unconventional areas.

Jingang Bai received the B.Sc. degree in Electrical Engineering from Harbin University of Science and Technology in 2009, and M.Sc. degree from Harbin Institute of Technology, in 2011, where he is currently working toward the Ph.D. degree. His research interests include flux-modulated brushless compound-structure PM synchronous machine used in hybrid electric vehicles, and high power density linear machines used in stirling engine system.

Pengfei Wang received the B.Sc. and M.Sc. degrees in Electrical Engineering from Harbin Institute of Technology, Harbin, China, in 2007 and 2009, respectively, where he is currently working toward the Ph.D. degree. His research interests include fault-tolerant permanent-magnet synchronous machines, permanent-magnet linear machines, and control strategies of multiphase machines under healthy and post-fault conditions.